The HKU Scholars Hub   The University of Hong Kong   香港大學學術庫

Title	Novel design of double-stator single-rotor magnetic-geared machines
Author(s)	Liu, C; Chau, KT; Zhang, Z
Citation	IEEE Transactions on Magnetics, 2012, v. 48 n. 11, p. 4180-4183
Issued Date	2012
URL	http://hdl.handle.net/10722/192185
Rights	IEEE Transactions on Magnetics. Copyright © IEEE.

Novel Design of Double-Stator Single-Rotor Magnetic-Geared Machines

Chunhua Liu, K. T. Chau, and Zhen Zhang

Department of Electrical and Electronic Engineering, The University of Hong Kong, Hong Kong, China

In this paper, the concept of double stators and the concept of magnetic gears are artfully integrated to form a novel class of machines. By utilizing the modulation-ring structure, the proposed machines can modulate the high-speed rotating armature field of the stators to match the low-speed rotating permanent-magnet (PM) field of the rotor. Hence, the machines readily achieve the low-speed high-torque merit. In addition, the fractional-slot structure can be adopted for the inner-stator design to remove the modulation-ring of the inner stator. Two possible machine structures are discussed and compared. Their characteristics and performances are calculated by using the time-stepping finite-element-method. The results well verify the validity of the proposed machine design.

Index Terms—Direct drive, double-stator machine, fractional-slot, magnetic gear, modulation-ring.

I. INTRODUCTION

RECENTLY, magnetic gears have attracted much attention because of their higher transmission efficiency, lower acoustic noise and maintenance-free operation over the mechanical gearboxes [1]. By incorporating the concept of magnetic gears into machines, the magnetic-geared machines take the definite merit for low-speed high-torque application [2], [3]. Meanwhile, the concept of double-stator machines is impressive since it offers higher torque density and better performance than its single-stator counterpart [4], [5].

The purpose of this paper is to propose a novel design for the magnetic-geared machines, which artfully incorporates the concepts of magnetic gears and double stators. The key is to utilize the modulation-ring to modulate the high-speed rotating armature field of the stators to match the low-speed rotating PM field of the rotor, hence achieving the low-speed high-torque merit. Also, the fractional-slot design will be utilized to simplify the proposed double-stator magnetic-geared (DSMG) machines. By using the time-stepping finite-element-method (TS-FEM), the machine characteristics and performances will be analyzed to assess the design validity.

II. MACHINE DESIGN AND OPERATION PRINCIPLE

A. Machine Design

The proposed DSMG machines are shown in Fig. 1, namely the dual-ring type which has two modulation-rings, and the single-ring type which adopts the fractional-slot structure with only one modulation-ring. Both machines adopt the same outer-stator structure, which has 6 slots to accommodate armature windings. Also, both machines have the same sandwiched rotor with two sets of 22 pole-pair PMs mounted on its inner and outer surfaces. Between the outer stator and the sandwiched rotor, a modulation-ring is adopted for both machines to modulate the magnetic field between the outer-stator and the sandwiched rotor. Meanwhile, they adopt different inner-stator topologies. The former adopts the same design as the outer-stator topology which consists of 6 slots and the modulation-ring. The latter utilizes the fractional-slot structure,
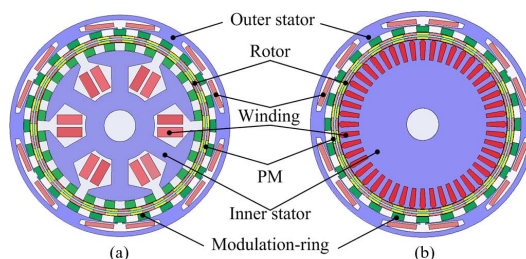
Fig. 1. Proposed DSMG machines. (a) Dual-ring type. (b) Single-ring type.

TABLE I
KEY DATA OF DSMG MACHINES

	Dual-ring type	Single-ring type
Rated speed	200 rpm	200 rpm
Outer stator outside diameter	280.0 mm	280.0 mm
Outer stator inside diameter	229.2 mm	229.2 mm
Inner stator outside diameter	210.0 mm	210.0 mm
Inner stator inside diameter	40.0 mm	40.0 mm
Rotor outside diameter	228.0 mm	228.0 mm
Rotor inside diameter	211.2 mm	211.2 mm
Inner and outer airgap lengths	0.6 mm	0.6 mm
Axial length	80.0 mm	80.0 mm
No. of outer stator slots	6	6
No. of inner stator slots	6	48
No. of rotor PM pole pairs	22	22
No. of modulation-ring segments	24	24
No. of outer stator turns/slot/phase	80	80
No. of inner stator turns/slot/phase	80	20

which makes use of 48 slots to correspond with 22 pole-pair PMs. Therefore, both machines can achieve the low-speed operation capability and high-torque output merit.

The design parameters of the proposed machines are listed in Table I. For a fair comparison, they are designed based on the following criteria:

- same outside diameter, shaft diameter and axial length;
- same outer stator and sandwiched rotor;
- same gearing ratio;
- same iron, copper and PM materials used.

B. Operation Principle

The torque transmission of both machines is based on the modulation of the airgap flux density distribution along the radial and circumferential directions. According to [1] and [2],
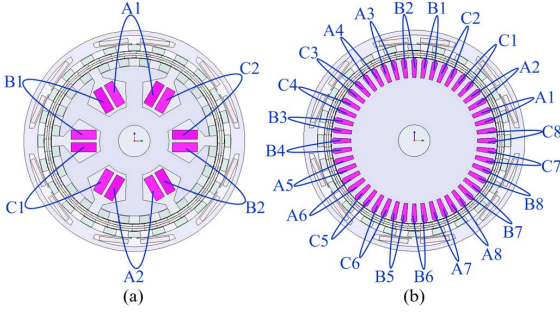
Fig. 2. Winding connections of inner stators. (a) Dual-ring type. (b) Single-ring type.

the airgap flux density space harmonics and the corresponding number of pole-pairs are, respectively, given by

$$\omega_{j,k} = \frac{jp_s}{|jp_s + kN_{ri}|}\omega_s, \quad p_{j,k} = |jp_s + kN_{ri}| \quad (1)$$

where $j = 1, 3, 5, \ldots$ and $k = 0, \pm 1, \pm 2, \ldots$, ω_s is the rotating field speed of the stator winding, p_s is the number of pole-pairs of the stator armature winding, and N_{ri} is number of modulation-ring segments. So, in order to transmit the torque from the armature field of the stator to the rotating field of the rotor, the rotor speed ω_r and the number of pole-pairs of the PM rotor p_r should be equal to $\omega_{j,k}$ and $p_{j,k}$, respectively. When $j = 1$ and $k = -1$, the largest space harmonic component is resulted for torque transmission.

For the dual-ring design, $p_s = 2$ and $N_{ri} = 24$ are selected. Then, it yields $p_r = 22$, and $\omega_s/\omega_r = 11/1$ which indicates that the rotor speed is 1/11 of the armature rotating field speed in the stator. Thus, when the armature rotating field in the stator is 2200 rpm, the rotor speed is scaled down to 200 rpm.

For the single-ring machine design, the fractional-slot structure can be utilized for the stator design. Its pole-pair arrangement is governed by

$$2p_r = N_s - 2p_{sf} \quad (2)$$

where N_s is the number of inner stator slots and p_{sf} is the number of pole-pairs of the armature winding. When the same number of rotor pole-pairs and the same number of stator rotating field pole-pairs are adopted, namely $p_r = 22$ and $p_{sf} = 2$, it yields $N_s = 48$. It indicates that the rotor can also provide the speed of 200 rpm when the rotating field of the armature winding is 2200 rpm.

Therefore, these two machines have the following features:

1) With the modulation-ring or fractional-slot structure, the proposed machines possess the magnetic gearing effect, hence achieving high torque at low speeds.
2) Since two sets of stator windings are used for both machines, the winding ends can be connected in versatile ways, hence providing EMF control under the same speed.
3) The modulation-ring is composed of iron segments and polyester segments. The iron segments can be made of laminated iron or iron powder. The laminated iron offers better performance than the iron powder but is more difficult for manufacture. The whole ring is adhered together by the polyester material, and then fixed at the
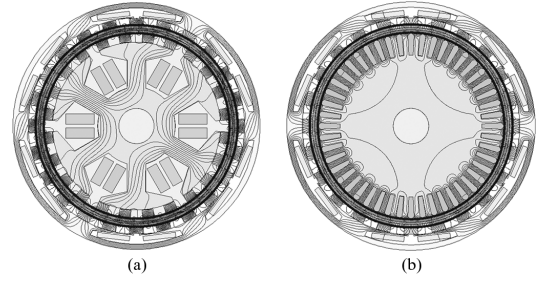

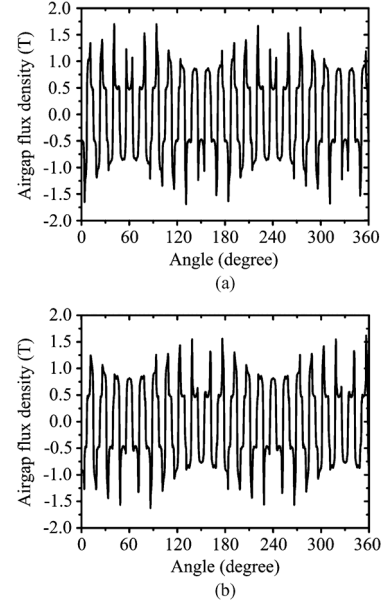Fig. 3. Magnetic field distributions. (a) Dual-ring type. (b) Single-ring type.

Fig. 4. Airgap flux density of dual-ring type. (a) Inner. (b) Outer.

machine frame so as to provide the desired stiffness for torque transmission.
4) The manufacturability is mainly affected by the mechanical integrity and precision of the rotor which is sandwiched between two stators. In order to ensure the integrity, the rotor can be designed as cup-shaped [4].
5) When the machines serve as generators, the rotor can be directly coupled with low-speed rotating devices for renewable energy harvesting, such as the wind turbines, to produce electricity.
6) When they work as motors, the rotor can be directly coupled with wheels for electric vehicles. Hence, the in-wheel direct-drive operation and independent wheel speed control can be achieved.

III. COMPARATIVE ANALYSIS

A. Structure Analysis

The major difference of both machines is their inner-stator topologies. Fig. 2 shows their winding connections. The dual-ring type follows the sequence of $+A - A + B - B + C - C + A - A + B - B + C - C$, whereas the single-ring type follows the sequence of $+A - A + A - A + C - C + C - C + B - B + B - B$, $-A + A - A + A - C + C - C + C - B + B - B + B$. Based on the winding arrangements, they have the following features:

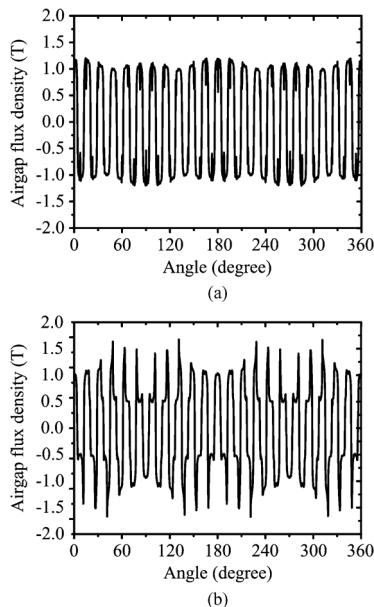1) The dual-ring structure can effectively reduce the number of stator slots and increase the slot space.

Fig. 5. Airgap flux density of single-ring type. (a) Inner. (b) Outer.

Fig. 6. No-load EMF waveforms of dual-ring type. (a) Separate. (b) Series.

2) The single-ring structure can enable the windings more uniform, and has relatively short end windings. However, the multi-slot structure increases the difficulty in winding coils and the manufacturing process.

3) Based on the torque transmission principle, the dual-ring structure utilizes the space harmonic component, whereas the single-ring one uses the fundamental component. So, the latter can produce higher torque than the former.

B. TS-FEM Analysis

First, the electromagnetic field equation of the proposed machines is governed by

$$\Omega : \frac{\partial}{\partial x}\left(v\frac{\partial A}{\partial x}\right) + \frac{\partial}{\partial y}\left(v\frac{\partial A}{\partial y}\right)$$
$$= -J - v\left(\frac{\partial B_{ry}}{\partial x} - \frac{\partial B_{rx}}{\partial y}\right) + \sigma\frac{\partial A}{\partial t} \quad (3)$$

where Ω is the field solution region, A the magnetic vector potential, J the current density, σ the electrical conductivity, and B_{rx}, B_{ry} the remanent flux density. Second, the machine armature circuit equation during motoring is given by

$$u = Ri + L_e\frac{di}{dt} + \frac{l}{S}\iint\limits_{\Omega_e}\frac{\partial A}{\partial t}d\Omega \quad (4)$$

where u is the applied voltage, R the winding resistance, i the phase current, L_e the end winding inductance, l the axial length, S the conductor area of each phase winding, and Ω_e the total cross-sectional area of conductors of each phase winding. Third, the machine motion equation is expressed as

$$J_m\frac{d\omega}{dt} = T_e - T_L - \lambda\omega \quad (5)$$

where J_m is the moment of inertia, ω the mechanical speed, T_e the electromagnetic torque, T_L the load torque, and λ the damping coefficient. After discretizing (3)–(5), the TS-FEM can readily be deduced [6].
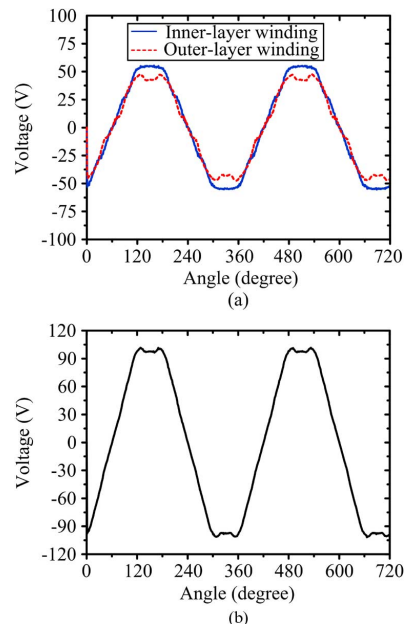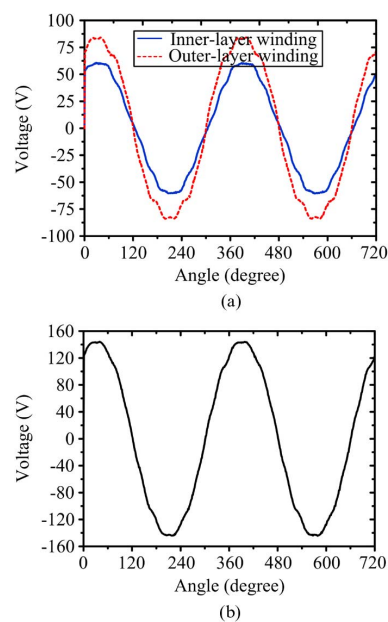

Fig. 7. No-load EMF waveforms of single-ring type. (a) Separate. (b) Series.

IV. PERFORMANCE COMPARISONS

Based on the TS-FEM, the machine characteristics and performance can be obtained. Fig. 3 shows the no-load magnetic field distributions of both machines. Hence, the corresponding airgap flux density distributions are deduced as shown in Figs. 4 and 5. It can be seen that the dual-ring type has similar patterns at the inner and outer airgaps, whereas the single-ring type has different patterns. Also, the single-ring one has a smoother inner airgap flux density distribution due to its fractional-slot structure. Their no-load electromotive (EMF) waveforms at 200 rpm are simulated as shown in Figs. 6 and 7 with and without connecting the inner- and outer-layer windings in series. As expected, the dual-ring type has two similar EMF waveforms, whereas the single-ring type offers different EMF waveforms
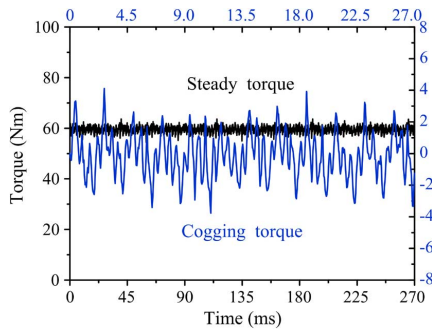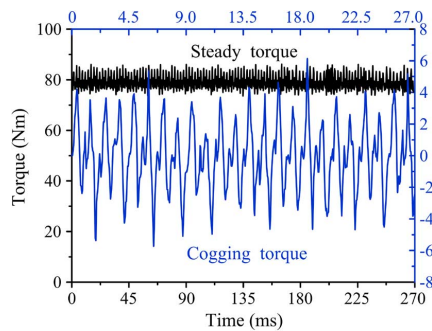
Fig. 8.   Torque waveforms of dual-ring type.

Fig. 9.   Torque waveforms of single-ring type.

Fig. 10.   Comparison of core losses at rated load.

TABLE II
MACHINE PERFORMANCE COMPARISON

	Dual-ring type	Single-ring type
Rated power	1215 W	1405 W
EMF amplitude at 200rpm	102.0 V	144.0 V
Rated torque	60.6 Nm	79.8 Nm
Torque density	12.3 kNm/m^3	16.2 kNm/m^3
Average shear stress	31.0 kPa	41.4 kPa
Torque ripple at rated power	13.2%	16.0%
Cogging torque / rated torque	7.2%	7.8%
Efficiency at rated power	85.9%	86.3%

with higher amplitudes. When connected in series, the corresponding amplitudes can achieve 102 V and 144 V, respectively.

Consequently, both the steady torque and cogging torque waveforms of the dual-ring type and single-ring type at rated load are simulated as shown in Figs. 8 and 9, respectively. They illustrate that their average steady torques are 60.6 Nm and 79.8 Nm, respectively, thus verifying that the single-ring type exhibits better torque performance. Meanwhile, their normalized torque ripples are 13.2% and 16.0%, respectively, which agree with the machine designs that the dual-ring type utilizes the space harmonics while the single-ring type makes use of the fundamental component. In addition, their cogging torques are only 7.2% and 7.8% of their steady torques, confirming that both machines have relatively small torque ripple and cogging torque.

Finally, core losses of both machines are analyzed. The core loss is calculated by using experiential equations, which include the fundamental and harmonic flux density components [7]. So, based on the flux density of the iron core resulted from the TS-FEM, the core loss can be readily determined. As shown in Fig. 10, the dual-ring type and the single-ring type have their average values of 65 W and 82 W, respectively. Taking into account the copper losses 134.4 W and 140.8 W at the rated current of 8 A for the rated powers of 1215 W and 1405 W, respectively, the machine efficiencies are 85.9% and 86.3%, respectively.

The overall performances of the proposed two machines are summarized in Table II.

V. CONCLUSION

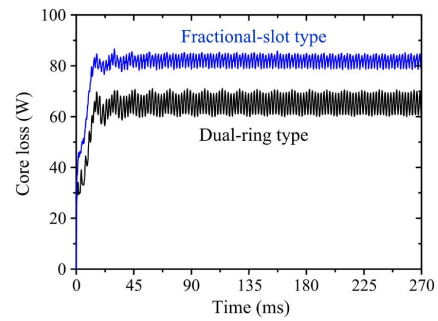This paper has presented a novel class of DSMG machines which include the dual-ring and single-ring structures. Because of the double-stator arrangement, they both achieve high torque density. Also, due to their magnetic gearing effect, they can offer high output torque under low speed operation. Between the two structures, the single-ring type provides higher torque density, but accompanies with larger torque ripple and cogging torque. On the contrary, the dual-ring type has a lower percentage core loss. Also, it is more simple for manufacturing.

REFERENCES

[1] K. Atallah and D. Howe, "A novel high performance magnetic gear," *IEEE Trans. Magn.*, vol. 37, no. 4, pp. 2844–2846, 2001.
[2] K. T. Chau, D. Zhang, J. Z. Jiang, C. Liu, and Y. Zhang, "Design of a magnetic-geared outer-rotor permanent-magnet brushless motor for electric vehicles," *IEEE Trans. Magn.*, vol. 43, no. 6, pp. 2504–2506, 2007.
[3] L. Jian, K. T. Chau, and J. Z. Jiang, "A magnetic-geared outer-rotor permanent-magnet brushless machine for wind power generation," *IEEE Trans. Ind. Appl.*, vol. 45, no. 3, pp. 954–962, 2009.
[4] S. Niu, K. T. Chau, J. Z. Jiang, and C. Liu, "Design and control of a new double-stator cup-rotor permanent-magnet machine for wind power generation," *IEEE Trans. Magn.*, vol. 43, no. 6, pp. 2501–2503, 2007.
[5] S. Niu, K. T. Chau, and C. Yu, "Quantitative comparison of double-stator and traditional permanent magnet brushless machines," *J. Appl. Phys.*, vol. 105, no. 7, pp. 1–3, 2009, paper no. 07F105.
[6] C. Liu, K. T. Chau, J. Z. Jiang, and S. Niu, "Comparison of stator-permanent-magnet brushless machines," *IEEE Trans. Magn.*, vol. 44, no. 11, pp. 4405–4408, 2008.
[7] C. Liu, K. T. Chau, and W. Li, "Loss analysis of permanent magnet hybrid brushless machines with and without HTS field windings," *IEEE Trans. Appl. Supercond.*, vol. 20, no. 3, pp. 1077–1080, 2010.